



LARGE-SIGNAL STABILITY OF AN INVERTER-BASED GENERATOR USING A LYAPUNOV FUNCTION

Brahm Pal Singh, Lecturer, Department of Electrical Engineering, IIMT Group of College, GreaterNoida-201310 bhrahm4257_gn@iimtindia.net , brahmpal.eee@gmail.com

Gopendra Kumar, Lecturer, Department of Electrical Engineering, IIMT Group of College, GreaterNoida-201310 gopendraiitd@gmail.com

Abstract

Due to the efficient operation of the DC system and the development of various DC loads, DC Microgrids became high power schemes. The stability of DC system is a major challenge for DC microgrids in addition to the traditional AC power system scheme. A stability analysis dc/ac inverter based generator model based on small signal but this technique is applied only for small disturbance microgrid system. In present scenario we will find and analysis stability of large disturbance based on large signal stability of a local generation power grid. Which grid connected to main grid for power may be export and may be power in port as per as local demand of power. According past studies of small disturbance on micro grid system based on the linearization technique. When small disturbance occurs in a micro grid system connected to main grid due to some dc input power from renewable energy sources that we will find attraction of region stability based on linearization mathematical model. But large signal stability analysis based on nonlinear technique. We find stability region closed to equilibrium point based on the lyapunov function. Lyapunove technique provides solutions of nonlinear system. Nonlinear systems are higher order system which gives good result if we reduce order of the system by neglecting some less sensitive variable parameter. First one we find the transfer function of inverter based generator model with controlling action and by using lyapunove technique for determine the asymptotic stability which provides zeros and poles location in x-y plane.

And finally we applied popov method and generate energy function for simulation on matlab for MATLAB/Simulink software is used to simulate the DC microgrid.

Keywords-- Microgrid, Inverter-based generator model, Electrostatic machine system, Energy function, Lyapunove function, popov's method, asymptotic stability, power system stability,

Introduction

A microgrid is a localized micro power system which operates as a single controllable system. It consists of a cluster of several distributed energy resources (DERs), energy storage devices and DC and AC loads. In DC microgrid, these all are connected to a common DC bus via converters. Units that produce AC will be connected to common DC bus via an AC-DC converter. A number of important research and developments are underway to integrate renewable energy sources into power distribution networks. Due to development of the power electronic devices, the renewable energy sources can be easily integrate with DC microgrid. Based on the type of connection, the microgrid can be DC microgrid, AC microgrid and Hybrid microgrid which is the combination of DC and AC microgrid [1-3].

In recent years the DC microgrid has become high energy source and superior power system because of higher efficiency of DC system. Many researches is to be done on the development of DC loads. DC microgrids have several advantages compared to AC microgrids. Key advantages of DC microgrid are that higher efficiency, more power transfer capacity, easy source connection to DC buses, and negligible power transmission losses. DC microgrids have a very wide potential for different power application, and it can be classified into different voltage levels: low-voltage DC (LVDC) and medium-voltage DC (MVDC). MVDC are rated 1500V to 22KV. MVDC microgrids are mainly used in marine vessels, data centers, aircraft, seas, and other sensitive loads and industrial applications [4]. LVDC microgrids are widely used in power system management, telecommunication,

residential and security systems[5].

1. TOOLS AND METHOD OF LARGE –SIGNAL STABILITY

Basically lyapunove technique provides stability region close top equilibrium point of higher order nonlinear system.

2. INVERTER-BASED GENERATOR MODEL OF MICROGRID

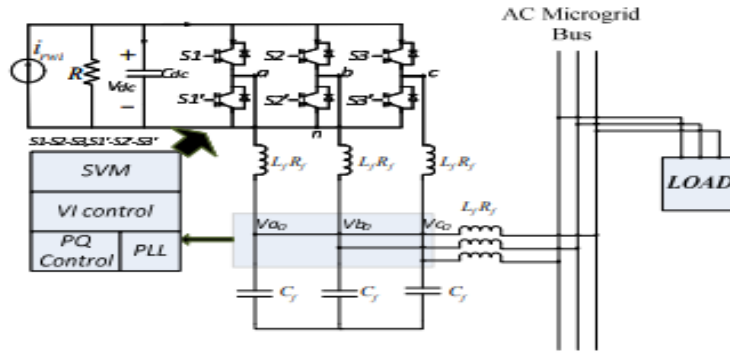


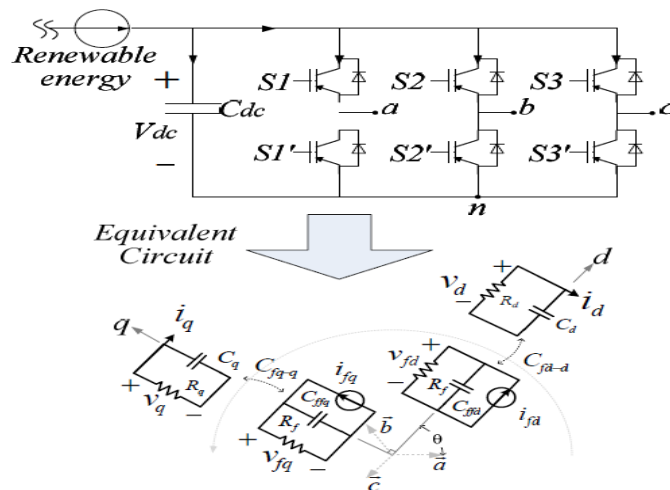
Fig 1: Inverter-based generator model of microgrid

1. Synchronous Generators

The electrostatic machine concept applied [13], the generator can be modeled. The generator electrical equivalent circuit is shown in Figure. 2.2 For the electrostatic machine concept the swing equation.

$$M \frac{d^2 \delta}{dt^2} + D \frac{d\delta}{dt} = p - p_e \tag{1.1}$$

$$M = \frac{2Hk_p w_y + 1}{k_p w_y}, \quad D = \frac{1}{k_p} \tag{1.2}$$



Above that equation is standardized in terms of the constant of inertia H per unit, defined as that of the "kinetic" energy in watt-seconds.

$$\frac{1}{2} C V_{dc}^2 = \frac{1}{2} J \omega_r^2 \rightarrow H = \frac{C V_{dc}^2}{2 V A_{base}} \tag{1.3}$$

That damping ratio is $H_i / \pi f$ By using the swing equation, this same actual energy can be evaluated

on the physical rotor, [18].

2 .Equivalent circuit of generator

An electrostatic machine's steady state study enables its corresponding circuit to still be modelled, its voltage , current and impedance values measured as well as the power flows from dc sources to grid by intelligent controlling interference.

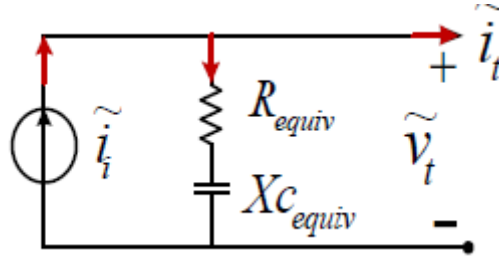


Figure.3.3

The current and voltage of the machine's stators can be expressed in equation 1.4

$$i_i = \frac{1}{X_{C_{fq-q}}} V_{fq} - j \frac{1}{X_{C_{fd-d}}} V_{fd} \quad (1.4)$$

The equivalent direct axis reactance's and quadratic voltage's equations are described on equation 1.5

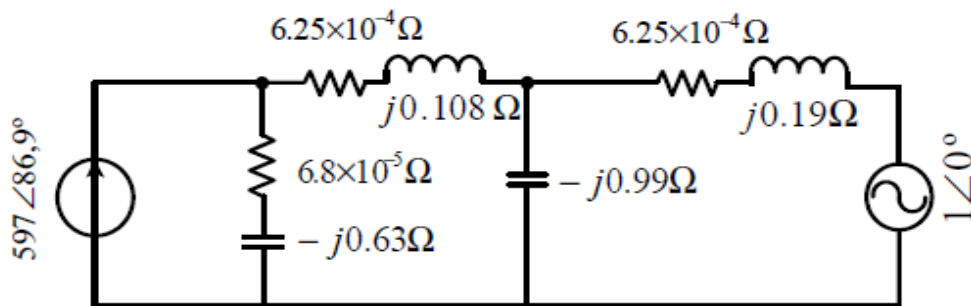
$$X_{C_{fd-d}} = X_{C_{fq}} = X_{C_{dc}} = (W_{C_{dc}})^{-1}$$

$$V_{fq} = \frac{V_{dc}}{2} d_q. V_{fd} = \frac{V_{dc}}{2} d_d \quad (1.5)$$

Here d is average inverter duty span. Finally, that resistance or reaction equivalents can be interpreted as follows, integrating the equations above:

$$X_{C_{equiv}} = X_{C_{dc}} \left(\frac{d_q^2 - d_d^2}{d_q^2 - d_q^2} \right)$$

$$R_{equiv} = X_{C_{dc}} \left(\frac{2d_q d_d}{d_q^2 + d_q^2} \right) \quad (1.6)$$



3. State-spaces modeling of the inverter-based model

The switching power converter may also be depicted in the form of (2.1) for switching mode with a switched state-space model.

$$\dot{x} = A_i x + B_i u \quad (2.1)$$

That switching power converter of switching mode with such a switched state-space model may also be depicted in (3.1)

$$X = \begin{bmatrix} i_L \\ V_C \end{bmatrix}, \quad u = v_{in} \quad (2.2)$$

Its system is generated assuming this same switching has been ideal throughout the regulated transistor T boost converter, as well as the diode voltage drop is zero. In continuous conduction situation the boost converter has two different working modes[20]. One mode is switch ON as well as the other mode is turn OFF. That switch is closed during 'ON' mode whereas the diode is open. Via V_{in} the inductor becomes charged. There is no current flowing from V_{in} to the condenser as well as the condenser discharges through the charging resistor. The equivalent circuit is merely two separate loops. We get the differential equations from current mode as (3.3) and (3.4)[10].

$$\dot{x}_1 = \frac{-R_L}{L}x_1 + \frac{V_{in}}{L} \quad (2.3)$$

$$\dot{x}_1 = \frac{-R_L}{L}x_1 + \frac{V_{in}}{L} \quad (2.3)$$

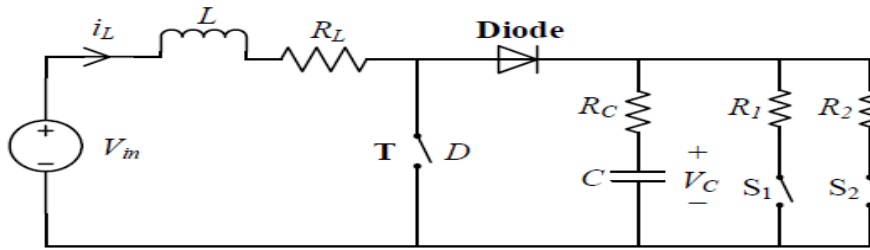


Figure 4.1. Actual circuit of the boost converter

Whenever the switch is OFF, the diode conducts, and also the voltage source starts to recharge its condenser and supply voltage again for charge. That system transitions to a new mode with such a series of differential equations defined in (2.5) and (2.6).

$$R_L x_1 + L \dot{x}_1 + R_C C \dot{x}_2 = V_{in} - x_2 \quad (2.5)$$

$$R_L (x_1 - C \dot{x}_2) = x_2 + R_C C \dot{x}_2 \quad (2.6)$$

By simple modification to the above equations.

$$A_{on} = \begin{bmatrix} \frac{-R_L}{L} & 0 \\ 0 & \frac{-1}{(R_C+R)} \end{bmatrix}, \quad B_{on} = \begin{bmatrix} \frac{1}{L} \\ 0 \end{bmatrix} \quad (2.7)$$

$$A_{off} = \begin{bmatrix} \frac{-R_C R_L + R(R_C + R_L)}{L(R+R_C)} & \frac{-R}{L(R+R_C)} \\ \frac{R}{L(R+R_C)} & \frac{-1}{(R+R_C)} \end{bmatrix} \quad (2.8)$$

$$B_{off} = \begin{bmatrix} 1 \\ \frac{1}{L} \\ 0 \end{bmatrix} \quad (2.9)$$

Due to line impedance is very low in DC microgrid, the fault current and fault current

4. Average model

That average state space model [6] could be computed based on the two-mode model above, if all the equations weighted by contribution time. These are given by duty ratio D as shown in (2.10) and (2.11)

above.

$$A_{av} = DA_{on} + (1 - D)A_{off} \quad (2.10)$$

$$B_{av} = DB_{on} + (1 - D)B_{off} \quad (2.11)$$

State-transition matrix (3.12) and (3.13) that can be used for later analysis

$$A_{av} = \begin{bmatrix} \frac{-R_C R_L + R(1 - D)R_C + R_L}{L(R + R_C)} & \frac{-(1 - D)R}{L(R + R_C)} \\ \frac{(1 - D)R}{L(R + R_C)} & -1 \\ \frac{1}{R + R_C} & 0 \end{bmatrix} \quad (2.12)$$

$$B_{av} = \begin{bmatrix} 1 \\ L \\ 0 \end{bmatrix} \quad (2.13)$$

The duty ratio D is now introduced in A_{av} . Therefore, the model is nonlinear [6].

3. LYAPUNOV STABILITY ANALYSIS

Lyapunov stability is one of the methods used to discuss differential equations which describe dynamic systems. Any Lyapunov function conditions will determine the system stability. Lyapunov's concept [24] of stability can be extended to high-order systems that aid in this topic containing a high-order microgrid system. To be asymptotically stable before any switching operation a switched system should have negative real parts of the proper values of the state transition matrix. The condition is equivalent to the following expression in the context of the linear space state model [10].

There exists Lyapunov equation as (3.19).

$$A^T P + P A = -Q \quad (2.19)$$

That corresponding Lyapunov function is defined as (3.20).

$$V(\tilde{x}) = \tilde{x}^T P \tilde{x} \quad (2.20)$$

The derivative of V is given as

$$\dot{V}(\tilde{x}) = -\tilde{x}^T Q \tilde{x} \quad (2.21)$$

For the system to be stable, the Lyapunov function $V(\tilde{x})$ must be certainly positive, radially unbounded and non-increasing. This can be expressed as

$$V(\tilde{x}) > 0, \forall \tilde{x} \neq 0 \quad (2.22)$$

$$V(0) = 0 \quad (2.23)$$

$$\dot{V}(\tilde{x}) \leq 0 \quad (2.24)$$

For such a switched linear system, it's also normal to consider quadratic common Lyapunov shape functions (3.20), so that we have definite symmetric Q for some positive

$$A_p^T P + P A_p \leq -Q, \forall p \in \mathcal{P} \quad (2.25)$$

However, Multiple Lyapunov functions can be used.

4. MULTIPLE LYAPUNOV FUNCTIONS.

Find the transfer function and check the stability performance of multi renewable energy sources are connected to inverter based generator model. For this transfer function we design state space model and applied Lyapunov technique.

$$\begin{aligned}\dot{\tilde{x}}_1 &= \widetilde{A}_1 \tilde{x}_1 \\ \dot{\tilde{x}}_2 &= \widetilde{A}_2 \tilde{x}_2\end{aligned}\quad (2.26)$$

That system are asymptotically stable, and let V1 and V2 be their Lyapunov functions respectively as

$$V_1(\tilde{x}) = \tilde{x}_1^T P_1 \tilde{x}_1, \quad V_2(\tilde{x}) = \tilde{x}_2^T P_2 \tilde{x}_2 \quad (2.27)$$

Clearly, stability becomes dependent mostly on switching signal for this switched system[13] as well as the Lyapunov-like function is partly continuous, as shown in Fig .. 3.2. That unit is switched every time after such a appropriate dwell period, such that the state becomes closer to the corresponding stable operating point.

4.1 Switching Condition for Guaranteed Instability

In time-dependent switching and state-dependent switching there's two forms of control methods. This was found also that time-dependent switching for both the boost converter was inefficient over a wide range of speeds, so it is instead using state-dependent switching here. As specified during last chapter As described in the last chapter, (V p) range(x range) range 0 is one of the conditions ensuring the system's stability with respect to a specific mode. That condition may help to get the inter-mode switch, too. The system becomes unstable if (V p) is 0 This can not happen in one mode since and mode is independently asymptotically stable..

However, the system is going to switch, there may be a condition for which $\dot{V}_p(\tilde{x}) = 0$,[12].

From mode 2 to mode 1 when

$$\left. \frac{dV_1}{dt} \right|_{\tilde{x}=\tilde{x}_2} = 0 \quad (2.28)$$

$$\Rightarrow \frac{\partial V_1}{\partial \tilde{x}_2} \cdot \frac{d\tilde{x}_2}{dt} = 0 \quad (2.29)$$

$$[(P_1 + P_1^T) \cdot \tilde{x}_2 + (P_1 + P_1^T) \cdot \Delta_s] \cdot (A_2 \cdot \tilde{x}_2) = 0 \quad (2.30)$$

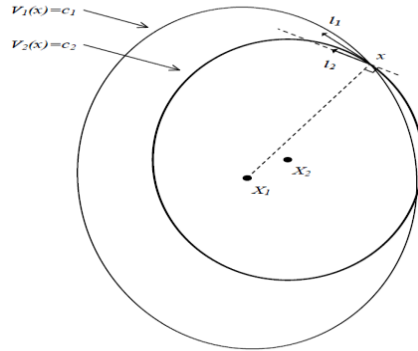
$$[(P_1 + P_1^T) \tilde{x}_1] \cdot ((A_2 \cdot \tilde{x}_2)) = 0 \quad (2.31)$$

Clearly, stability becomes dependent mostly on switching signal for this switched system[13] as well as the Lyapunov-like function is partly continuous, as shown in Fig .. 3.2. That unit is switched every time after such a appropriate dwell period, such that the state becomes closer to the corresponding stable operating point.

5. SWITCHING CONDITION FOR GUARANTEED INSTABILITY

In time-dependent switching and state-dependent switching there's two forms of control methods. This was found also that time-dependent switching for both the boost converter was inefficient over a wide range of speeds, so it is instead using state-dependent switching here. As specified during last chapter As described in the last chapter, (V p) range(x range) range 0 is one of the conditions ensuring the system's stability with respect to a specific mode. That condition may help to get the inter-mode switch, too. The system becomes unstable if (V p) is 0 This can not happen in one mode since and mode is independently asymptotically stable..

However, the system is going to switch, there may be a condition for which $\dot{V}_p(\tilde{x}) = 0$,[12].



5.1 Equilibrium region of the System

Equilibrium region can also be expressing by derivatives of both the function as zero. In that same way, the input power of the DC link for the generator is equal to the AC power supplied to the grid by the generator ($P_1 = P_{e1}$). That obtained equation expresses the relation between each generator's angles. Solve most of these equations.

The intervals from π to $-\pi$ are as follows:

$$P_e = \sqrt{F_{12}^2 + G_{12}^2} \sin\left(\delta_1 - \delta_2 + \tan^{-1}\left(\frac{F_{12}}{G_{12}}\right)\right) \quad (3.4)$$

$$(i) \quad \delta_1^s - \delta_2^s = \sin\left(\frac{P_e}{\sqrt{F_{12}^2 + G_{12}^2}}\right) - \tan^{-1}\left(\frac{F_{12}}{G_{12}}\right) \quad (3.5)$$

$$(ii) \quad \delta_1^u - \delta_2^u = \pi - \sin\left(\frac{P_e}{\sqrt{F_{12}^2 + G_{12}^2}}\right) - \tan^{-1}\left(\frac{F_{12}}{G_{12}}\right) \quad (3.6)$$

5.2 Transfer function of the stable equilibrium point to the origin

In Lyapunov stability problems, that microgrid's mathematical model becomes moved from the stable point of equilibrium to the point of origin, and use the transformation $y = \delta - \delta^s$. The representation of the state variables can be formulated as follows[10]

$$y_2 = \delta_{12} - \delta_{12}^s, \quad y_1 = \omega_1$$

$$\begin{cases} \frac{dy_1}{dt} = \frac{-D}{M} y_1 - \frac{1}{M} f(y_2) - \frac{1}{M} g(y_2) \\ \frac{dy_2}{dt} = y_2 \end{cases} \quad (3.7)$$

$$f(y_2) = F_{12}[\sin(y_2 + \delta_{12}^s) - \sin(\delta_{12}^s)]$$

$$g(y_2) = G_{12}[\cos(y_2 + \delta_{12}^s) - \cos(\delta_{12}^s)]$$

All state space parameter can be expressed in matrix formulation as:

$$\dot{Y} = AY - B_1 f(y_2) - B_2 g(y_2)$$

$$A = \begin{bmatrix} -\lambda & 0 \\ 1 & 0 \end{bmatrix} B_1 = \begin{bmatrix} 1 \\ M_1 \\ 0 \end{bmatrix} B_2 = \begin{bmatrix} 1 \\ M_1 \\ 0 \end{bmatrix}$$

This is parameter of state space model. We can find the transfer function with the help of state parameter and we can generate energy function with the help of Popov method .this energy function provided helped in dspace plan.

$$f(y_2) = F_{12}[\sin(y_2 + \delta_{12}^s) - \sin(\delta_{12}^s)]$$

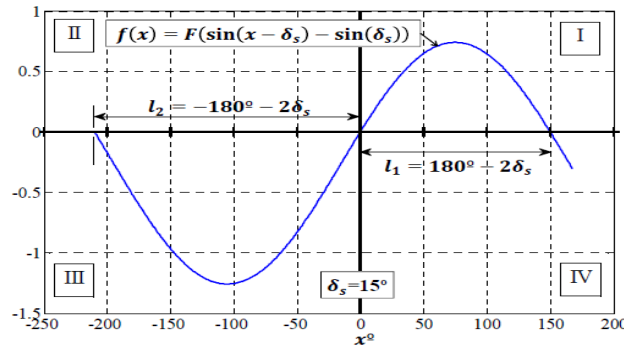


Figure.4.4 Nonlinearity of function f(x)

6. CASE STUDIES OF INVERTER-BASED GENERATOR

In view of the inductive nature of the network between some of the generators, I i.e. $ZB = \pi/2$ therefore the values of the G12 parameters becomes equal to zero. As just a consequence of this consideration the method could be expressed in (13) as shown in Fig. Four.2.[8] [10].

$$W(s) = C(SI - A)^{-1}B_1$$

That generator was simulated and depicted as just a block diagram (presented in Fig. 4.2 as a linear transfer function as well as a non-linear feedback path feature).

Where in the first and third quadrants of Fig lies the nonlinear function. 3.3, therefore the Lyapunov function can also be developed using a systematic technique One of the most commonly used systematic methods has become the Popov method. This method allows for the development of the Lyapunov function and the establishment of an attraction region for the equilibrium point. A moderate device without loss of energy is seen as the most critical scenario possible to detect limits of the equilibrium area of the generator.

6.1 Mathematical Boundary condition of Lyapunov function:

$$V(y_1, y_2) = \frac{1}{2}My_1^2 + \int_0^{y_2} f(u) du$$

$$V(y_1, y_2) = \frac{1}{2}My_1^2 F_{12}[\sin(y_2 + \delta_{12}^s) - \sin(\delta_{12}^s)] \quad (4.9)$$

Lyapunov satisfied the following properties:

- $V(0) = 0$;
- $V(y_1, y_2) > 0$ for all y_1, y_2
- $\frac{d}{dt}V(y_1, y_2) \leq 0$ along all trajectories of the system .

Then the point $(y_1, y_2) = 0$ is locally stable.

This should lie on the first and third quadrants as per the initial condition of function f(x). Which method is used to identify the region of attraction, to calculate angles 11 and 12 of the Lyapunov

equation, and also to determine the minimum values of equation taken among these angles. From the above measurements, this can be observed that any angle value determined by the Lyapunov techniques higher than that of the limit (11 or 12) would go beyond the area of attraction and create an unstable system state.

That study of the generator connected to a Microgrid will also be addressed in the next step, finding the region of stability for the device[9].

Simulations model

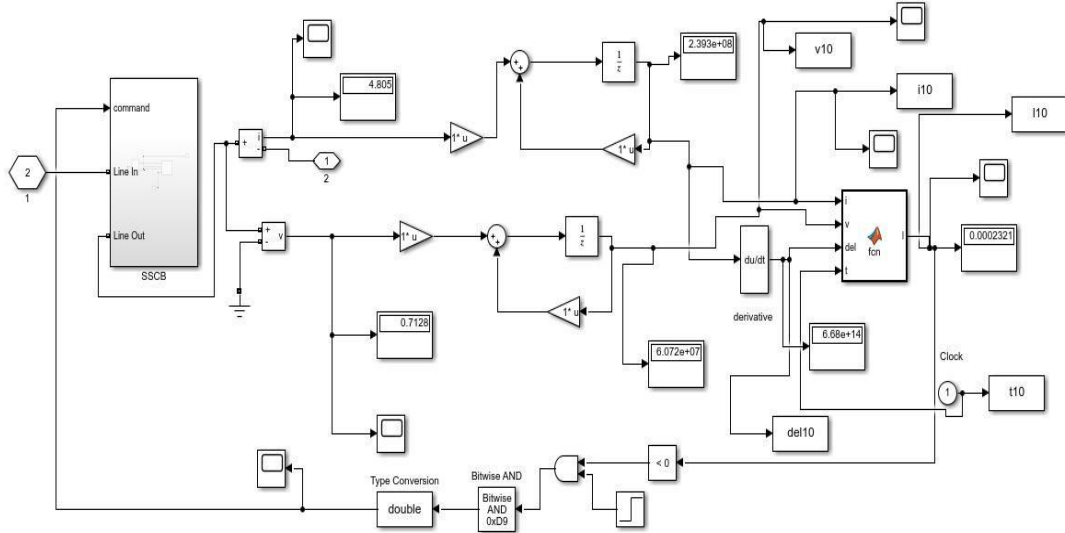


Figure- Complete MATLAB simulink model.

Simulations hardware - based in that Loop (HIL) are performed using d-SPACE ds1006, MATLAB / Simulink [16].

6.2 Simulation setup parameter of model

Type	Parameter	value
Electrical setup	DC voltage (Vdc)	650V
	AC voltage (Vac)	311V
	AC frequency (fr)	50Hz
	DC capacitance(Cdc)	5000µF
	AC fitter capacitance (Cf)	25 µF
	AC filter impedance(Lf)	1.8mH
Inner loop	Active droop control(KP)	0.00001W/rad
	Reactive droop control(KQ)	0.0001vAr/rad
	Virtual Resistance(Rv)	0.1Ω
	Virtual inductance(Lv)	4mH

Table:

- Stable equilibrium point;; $\delta_s = 1.5213$
- Unstable equilibrium point: $\delta_s = 1.6245$

To evaluate stability and region of conversion of these model using the technique of Lyapunov it is important to locate the model at its stable point of equilibrium. Using the electrostatic principle, the model on its constant states can be expressed as follows.

6.3 Simulation results analysis

Which demonstrate their efficacy of the switching technique, a MATLAB Simulink model was developed to graph those trajectories states space through application of the state dependent switching surfaces. That boost converter's linearized state-space model, extracted in Section II, was utilised as just a research target.

A look at objectivity. The method of simulation runs as per the parameters shown in the table below. Device parameter those are given in Table 4, and Table shows their two modes in the simulation. Both curves of the switching surfaces are determined in matlab software according to the Simulink simulation. Simulation split down into two sections[16].

Three simulations have been carried out under the 0.5 duty ratio but three separate load sets during the first section. This measures the device's instabilities whenever the different stable loads vary.

That duty ratio is reduced to 0.1, in the second part, and the fee has also increased. This is to verify the job ratio impact on system instability. Owing to the actual characteristics of its functional structure the states do not need to hit infinity

When both the inductance current and condenser voltage are negative, the boost converter may fail to operate and the assumptions of linearization fail. Because the condenser voltage limit is the most unstable too maintain because almost no negative capacitor voltage can be allowed, their stability condition could be interpreted as the following where I_m is the device's maximum current value, and V_{rms} is the maximum stable state voltage.

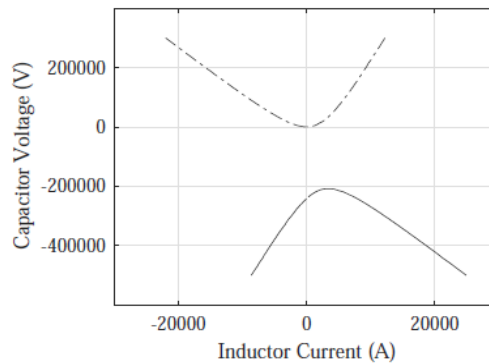


Figure.5.3

$$I \in [-I_m, I_m] \text{ and } V \in (0, 2V_{ms}) \tag{3.32}$$

6.4 Simulation I: Instability (Light Loads).

The output voltage of inverter is $V_o = \frac{V_s}{(1-D)}$ 400V without MATLAB simulation. The initial condition of the system state is $I = 20A$, $V = 390v$,

Each motion surface is also an ellipse, and another is the upper hyperbola branch shown in Fig. 4- at the two stable points are so similar to each other, that they are nearly coincident. The two black dots mark the stable status points, as shown in Fig.4.4. That there are two curves to both the surfaces that pass. The trajectory goes in anticlockwise direction.

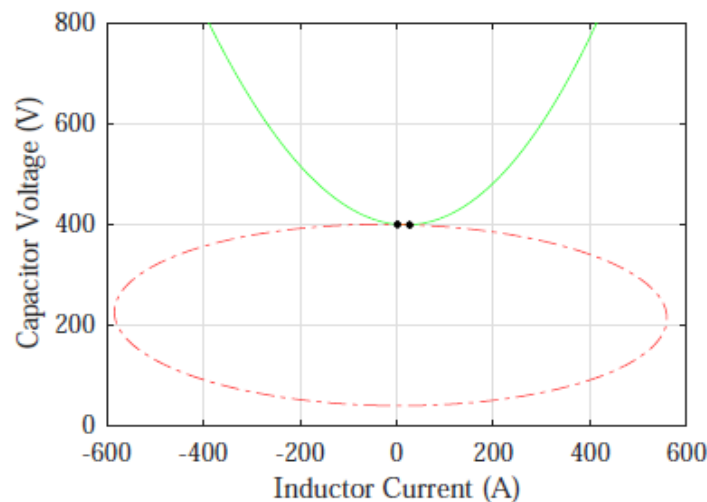


Figure.5.4

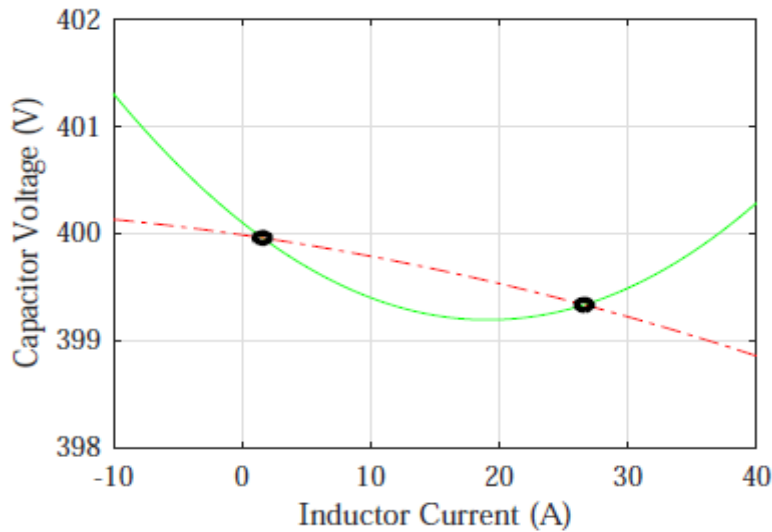


Figure.5.4

With all that in mind we describe a little further that initial level. The trajectory in Fig.4.6 shows back to a conclusion that the unit oscillation becomes strong so that the current of inductance rapidly becomes negative but we can still accept it. Mostly in trajectory it also is shown that the condenser voltage eventually reaches the zero axis,

6.5 Simulation II: Instability (Heavier Loads).

Each time that charge on the machine adjusted to be just a little heavier than the first simulation. The starting point becomes similar to the following. That difference would be that it determines the upper switching curve to become a parabolic like the Fig. 4.7 That lower curve resembles the ellipse, too. As shown in Fig. 4.6, the machine becomes unstable again. And provide descriptions of shape of the switch diagram. Additional load conditions fall into one or a third group, where the parabolic surface becomes an ellipse[16].

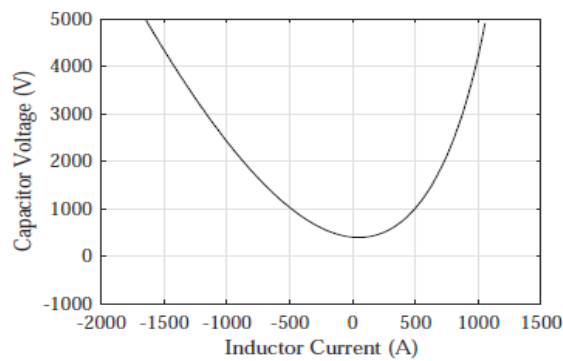


Figure.5.6

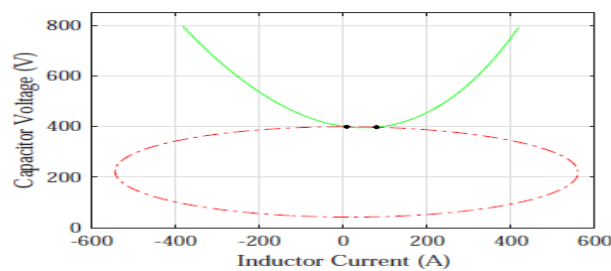


Figure.5.7

6.5 Simulation III: Stability.

In either case, their switching flags were adjusted in such a way that the switching only can take place

whenever the trajectory reaches the switching curves from the opposite end from which it reached in previous cases Fig. 4.8 Shows that case without shifting power, because the damping mechanism becomes weak and it takes a long time to settle. Fig. Fig. 4.9 The moving case-control displays and the computer became clearly much easier to dampen. It can best be seen in Fig. 3.10----Fig. 3.11 That's Good. They demonstrate how the Vs (blue solid line) and 2 states Working throughout Lyapunov. That Lyapunov function as we've seen, its Lyapunov function transformed more easily throughout the regulated case of switching than those in the uncontrolled case in Fig.4.10[24]

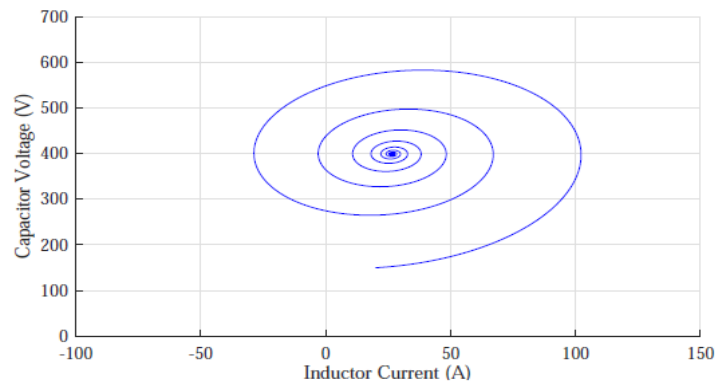


Figure.5.8.stability region for light load

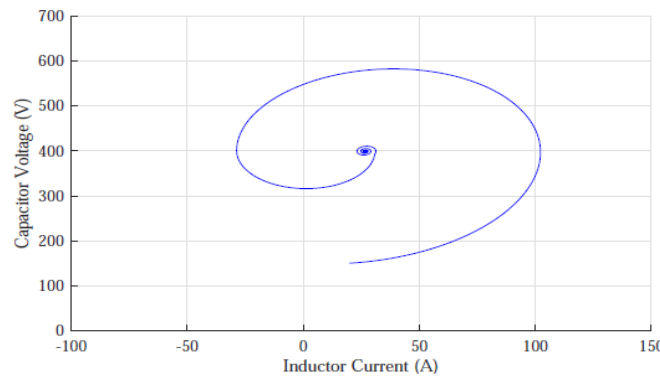


Figure.5.9.stability region for high load

CONCLUSION AND FUTURE SCOPE

The following conclusions are drawn below:-

- 1) A DC ring microgrid and stability system is simulated with the help of MATLAB/Simulink platform.
- 2) The stability with ring configuration of DC microgrid is a very complex system. It is challenge to obtain required reliability. Due to bidirectional power flow and current limiting control, its stability is challenging.
- 3) In this work, parameter estimation based on lyapunov and Popov technique is proposed to calculate the stability closed to equilibrium point in sable region.
- 4) In this approach find out stability of higher order system. These systems have maximum number of variables and it can solve easily by using lyapunov method.
- 5) That microgrid model throughout this dissertation becomes comparatively low such that parameters like electrostatic and swing equations. PI controller parameters can easily become stable in the network. More relevant would be the method of guaranteeing stability
- 6) It was explained that the microgrid system gives satisfactory results under variation in load, with frequency constant after a given time. Wind, solar photovoltaic, etc. systems can be used widely to meet energy demands adequately
- 7) From the simulation results it can be developed that the power supplied from the inverter-based



generator can effectively satisfy the variations in the demand for load power, and that the deviation in the system frequency is also properly controlled to be within a very restricted range.

- 8) The conventional PI controllers are commonly used for controlling purposes but the simulation results showed that the proposed PI controller provides better performance compared to conventional controllers due to extreme disturbances and significant disturbances in parameters of the environment and equipment

Future scope

1. This proposed protection scheme can be analyzed with different mode of operation such as grid-connected mode.
2. To reduce order of the transfer function for large signal stability by varying switching pulse with of control action or use any controller.

References

3. Mi Y., Fu Y., Li D., "The sliding mode load frequency control for hybrid power system based on disturbance observer," *Electrical Power and Energy Systems* 74 (2016) 446–452.
4. R. M. Kamel and K. Nagasaka, "Design and Implementation of Various Inverter Controls to Interface Distributed Generators (DGs) in Micro Grids," *Japan Society of Energy and Resources*, Session 6.1, 2009, pp. 60-64
5. the IEEE Industrial Electronics Society, pages 4385–4390, Nov 2009.
6. J. Belikovab and Y. Levronc. Comparison of time-varying phasor and dq0 dynamic models for large transmission networks2017 *International Journal of Electrical Power and Energy Systems*, pages 65–74, Dec 2017
7. R..H. Lasseter and P. Paigi. Microgrid a conceptual solution. In 2004 IEEE 35th Annual Power Electronics Specialists(IEEE Cat. No.04CH37551), volume 6, pages 4285–4290 Vol.6, June 2004
8. T.LVandooran, J. C. Vasquez, J. De Kooning, J. M. Guerrero, and Vandeveld. Microgrids: Hierarchical control and an overview of the control and reserve management strategies. *IEEE Industrial Electronics Magazine*, 7(4):42–55, Dec 2013.
9. A.Q. Huang. Medium-voltage solid-state transformer: Technology for a smarter and resilient grid. *IEEE Industrial Electronics Magazine*, 10(3):29–42, Sept 2016.
10. J.A. Mueller and J. W. Kimball. Generalized average modeling of dc subsystem in solid state transformers. In 2017 IEEE Energy Conversion Congress and Exposition ECCE), pages 1659–1666, Oct 2017
11. B.B. Johnson, A. Davoudi, P. L. Chapman, and P. Sauer Microgrid dynamics characterization using the automated characterization using the automated of 2010 IEEE International Symposium on Circuits and Systems, May 2010
12. Daafauz, P. Riedinger, and C. Iung. Stability analysis and control synthesis for switched systems: a switched lyapunov function approach *Stability analysis and control synthesis for IEEE Transactions on Automatic Control*, 47(11):1883–1887, Nov 2002
13. D.Liberzon and A. S. Morse. Basic problems in stability and design of switched systems. *IEEE Control Systems*, 19(5):59–70, Oct 1999.
14. D. Liberzon. *Switching in Systems and Control*. Birkhauser, Boston, 2003.
15. G.G. Karady, A. Q. Huang, and M. Baran. Freedom system: An electronic smart distribution grid for the future. In PES T D 2012, pages 1–6, May 2012.